Int. J. Electrochem. Sci., 15 **(2020)** 10453 – 10462, doi: 10.20964/2020.10.01

International Journal of ELECTROCHEMICAL SCIENCE
www.electrochemsci.org

Preparation of Cu_2S@ $Li_4Ti_5O_{12}$ Composite Electrode with Excellent Lithium Storage Performance by Spray Drying Reaction

Yingjie Zhang, Qian Feng, Xue Li[*]

National and Local Joint Engineering Laboratory for Lithium-ion Batteries and Materials Preparation Technology, Faculty of Metallurgical and Energy Engineering, Kunming University of Science and Technology, Kunming 650093, PR China
[*]E-mail: 438616074@qq.com

Received: 26 May 2020 / *Accepted:* 21 July 2020 / *Published:* 31 August 2020

In this work, spherical lithium titanate was prepared by spray drying. Then, copper particles were deposited on the lithium titanate using a copper mirror reaction. Finally, the composite was vulcanized to produce Cu_2S@$Li_4Ti_5O_{12}$ materials (named Cu_2S@LTO). As a coating layer capable of lithium storage, Cu_2S can effectively improve the conductivity and lithium storage capacity of lithium titanate materials. Improving the low conductivity of lithium titanate increases its specific capacity. Morphological and structural analyses show that the prepared composite material has a spherical structure and that Cu_2S is uniformly dispersed on the surface of the spherical particles with a high degree of crystallinity. In addition, the electrochemical performance of the lithium-ion battery cathode material Cu_2S@LTO in an ether electrolyte and ester electrolyte (LB303) was studied. The results show that the Cu_2S@LTO anode material has a better electrochemical performance in the ether electrolyte than that in the ester electrolyte. The first specific capacity reaches 206 mA h/g. The capacity retention rate is 91% after 30 cycles. Even at a high rate, the capacity retention rate after 100 cycles can still be maintained at 98.5%. The excellent electrochemical energy source is due to the synergistic effect of Cu_2S and lithium titanate, which not only improves the conductivity and specific capacity of lithium titanate but also effectively relieves the volume expansion of Cu_2S during lithium storage, thereby extending the battery cycle life.

Keywords: Lithium titanate modification; spray drying; copper mirror reaction; lithium-ion battery

1. INTRODUCTION

Lithium ion batteries are favored in the new energy industry due to their advantages of high operating voltages, large energy densities, and long cycle lives [1-3]. At present, graphite is the main material of lithium-ion battery anodes in the market. However, there are several problems associated with graphite anodes [4]. First, the lithium ion diffusion coefficient of graphite is low, and the rate performance is not ideal. Second, because the graphite anode material expands in volume during lithium intercalation, its cycle life is poor. Moreover, because the detachable potential platform of graphite anode materials is 0.1-0.15 V, its safety performance is not good. Compared with graphite anodes, the unique structure of titanium-based materials and the mechanism of lithium intercalation and deintercalation make them have many advantages in terms of electrochemical performance. For instance, during the intercalation and deintercalation of lithium, the lattice constant of titanium-based materials is almost unchanged, the volume change is close to zero, and the electrochemical reversibility is good. Titanium-based materials have a high potential platform of 1.55 V (vs. Li^+/Li) [5-7], making it difficult to produce lithium dendrites and resulting in a good safety performance. The lithium ion diffusion coefficient is higher in titanium-based materials than in other anode materials. Thanks for these advantages, lithium titanate has attracted much attention. However, lithium titanate still has the disadvantage of having a low conductivity and poor high-rate performance. Therefore, these factors hinder the large-scale application of lithium titanate [8,9].

At present, the following are the main ways of improving the conductivity and rate performance of lithium titanate [10-15]: (1) Synthesizing nanometer-sized lithium titanate materials can effectively shorten the diffusion path of Li^+, slow down electrode polarization, and, at the same time, increase the contact area between the electrode active material and the electrolyte. (However, due to the high surface energy, great surface activity, and extreme instability of nanoparticles, long-term cycling is not ideal). (2) A highly conductive phase coating enhances the electronic conductivity between the main separated particles to improve the conductivity of the composite electrode. Commonly used highly conductive phase coating modification methods include high-energy ball milling methods and solid-phase methods. (However, most of the conductive phases prepared by these methods are on the surface of the lithium titanate material or distributed around the particles and cannot be in close contact with the lithium titanate particles, which limits the improvement in the electrochemical performance). (3) Ion doping the crystal structure and doping metal ions at the Li^+ or Ti sites increases the electronic conductivity of the material itself and reduces the resistance of the electrode material. (However, due to the high surface energy, great surface activity, and extreme instability of nanoparticles, long-term cycling is not ideal).

In summary, the three modification methods have their own advantages and disadvantages. This work proposed a multi-effect modification method. Combined with the advantages and disadvantages of the nanometer particle size of the material, a micro-nano structure is fitted into a lithium titanate material, which ensures a high electrochemical activity and cyclic stability. Because Cu_2S has good electrical conductivity and excellent energy storage performance. Cu_2S can be combined with titanium-based materials to improve the electrochemical properties. In our previous work, a flexible, uniform $CuS_x@TiO_2$ composite electrode was prepared by electrophoresis combined with vulcanization at high temperature. The electrochemical tests show that the prepared flexible $CuS_x@TiO_2$ composite electrode has a good electrochemical performance. The coulombic efficiency can be maintained above 98% at a high current density of 400 mA g^{-1}. After 80 cycles, the reversible capacity can still reach 380.1 mAh g^{-1} [16]. In the other works we published, it is found that the electrolyte composition, ratio and electrolyte molecular structure have a significant impact on the energy storage behavior of copper sulfide compounds. The Cu_2S anode materials have the best cycling performance in 1 M LiTFSI DOL/DME =

1:1 v/v ether electrolyte and the worst electrochemical performance in 1 M LiTFSI DOL/DME = 7:3 v/v ether electrolyte [17, 18]. In this work, combine with the previous work experience, the conductive phase metal sulfide Cu_2S with a lithium storage activity is used as a coating layer to increase the weight specific capacity of the composite material and, in the meantime, improve the conductivity. The final prepared $Cu_2S@Li_4Ti_5O_{12}$ material combines the synergistic effect of the two individual materials, which not only improves the specific capacity of the material but also effectively relieves the volume expansion of Cu_2S during lithium storage, thereby extending the battery cycle life. The electrochemical behavior of the material in carbonate-based electrolytes and ether-based electrolytes was also detected.

2. EXPERIMENT

2.1 Preparation of materials

The method used to synthesize the spherical $Li_4Ti_5O_{12}$ material by spray drying is as follows: 6 g of tetrabutyl titanate was dissolved in 20 mL of deionized water and stirred for 5 min. Then, 15 g of 30% hydrogen peroxide was added, and a certain amount of 12.5% ammonia in water was added to adjust the pH to approximately 10. After 20 min, the white solution turned yellow-green. A certain amount of 96.0% lithium hydroxide was added, and the mixture was stirred for 2 h. Then spray drying was performed with an inlet temperature of 190 ℃, pressure of 0.2 MPa and feed rate of 650 mL/h. Finally, the precursor obtained by spray drying was burned in a muffle furnace at 700 ℃ for 16 h to obtain well-crystallized LTO.

A copper mirror reaction was used to deposit elemental Cu on LTO, and then, an NaOH solution was used to adjust the pH value of the mixture of copper sulfate and potassium sodium tartrate to between 11.5 ~ 12.5. Then, a certain amount of formaldehyde solution was added to reduce Cu^{2+}, and a certain proportion of LTO was stirred overnight and filtered to obtain the Cu@LTO material.

The Cu@LTO material was mixed with sulfur powder, calcined in an argon atmosphere, and sintered at 400 ℃ for 4 h to obtain the Cu_2S@LTO or CuS@LTO material.

2.2 Material characterization

Phase analysis of the samples was performed by X-ray diffraction (XRD). This article uses the Rigaku MiniFlex600X pet X-ray diffractometer (Japan), and the scanning speed is 4°/min. Scanning electron microscopy (SEM) was used to observe and analyze the surface morphology and particle size of the material, and the composition of the micro area was determined with a scanning electron microscope. This article uses a Hitachi S-4800 microscope and X-ray energy scattering analyzer produced by Japan Rigaku.

2.3 Electrochemical measurements

The CR2016 button cell was assembled in an argon atmosphere by using a lithium sheet as a symmetrical electrode. A porous polypropylene resin membrane is used as a separator between the two electrodes. The negative electrode material is made of 80 wt% active material, 10 wt% acetylene black (super P) and 10 wt% polyvinylidene fluoride (PVDF). The solvent is an oily solvent, n-methylpyrrolidone (NMP). Under the constant temperature condition of 25 °C, the test voltage range is 0.01 ~ 3.0 V (vs. Li/Li^+), and a LAND battery test system was used to determine the constant current charge and discharge cycle performance. A Princeton P4000 electrochemical workstation was used for cyclic voltammetry (CV), in which the scanning speed was 0.1 mV/s and voltage range was 0.01 ~ 3 V, and 5 cycles were performed.

3. RESULTS AND DISCUSSION

Figure 1 is the XRD pattern of Cu_2S@LTO, and the scanning range is 10° ~ 90°. It can be seen from Figure 1 that the characteristic peaks at 2θ = 18 °, 35 °, 43 °, 47 °, 57 °, 62 °, 66 °, 74 °, 79 °, and 82 ° correspond to the (111), (311), (400), (331), (333), (440), (531), (533), (444), (551) crystal planes of $Li_4Ti_5O_{12}$, respectively (JCPDS: 49-0207). The other characteristic peaks of this material correspond to the characteristic peaks of Cu_2S; there are no other peaks, and the peak shape is sharp, which proves that the product has a high purity and high degree of crystallinity.

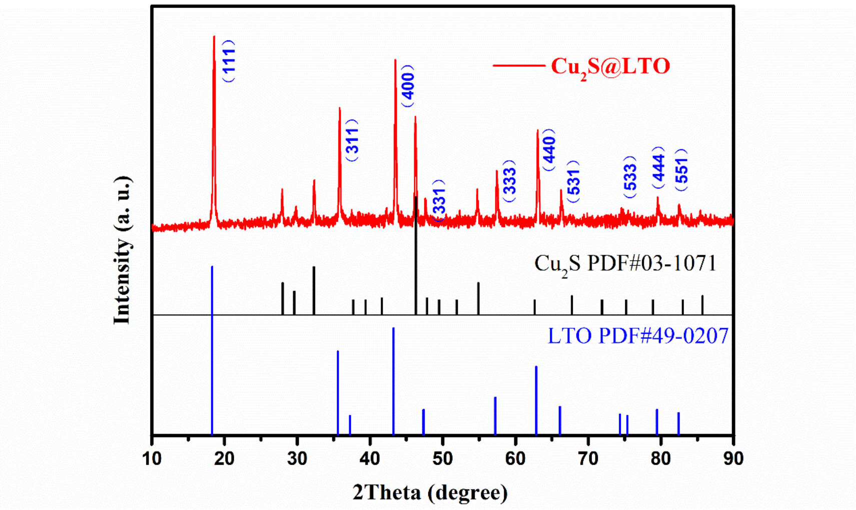

Figure 1. XRD patterns of Cu_2S@LTO

Figure 2 is a scanning electron micrograph of the $Li_4Ti_5O_{12}$ material prepared by spray drying and $Li_4Ti_5O_{12}$ coated with Cu_2S. Figure 2(a),(b) shows the micrograph of LTO. The surface of LTO is rough, the primary particle size is uniform, with particle sizes of approximately 50-150 nm, and the secondary particle size is approximately 2-6 µm. Figure 2(c),(d) is the SEM image of Cu_2S@LTO; the Cu_2S@LTO surface is rough, the primary particles are evenly distributed, and the particle size is approximately 150 nm to 300 nm. The secondary particle size is approximately 1- 3 µm, with slight agglomeration. After the LTO is coated with Cu_2S, the surface is rough, the primary particles become larger, and the morphology is still spherical. The element type and content of the surface of the Cu_2S@LTO material were analyzed by EDS, and it was found that Cu and S were present with a Cu:S ratio of 1.73, which was similar to the stoichiometric ratio of Cu_2S. It can be further proved that Cu_2S has been well coated on the LTO.

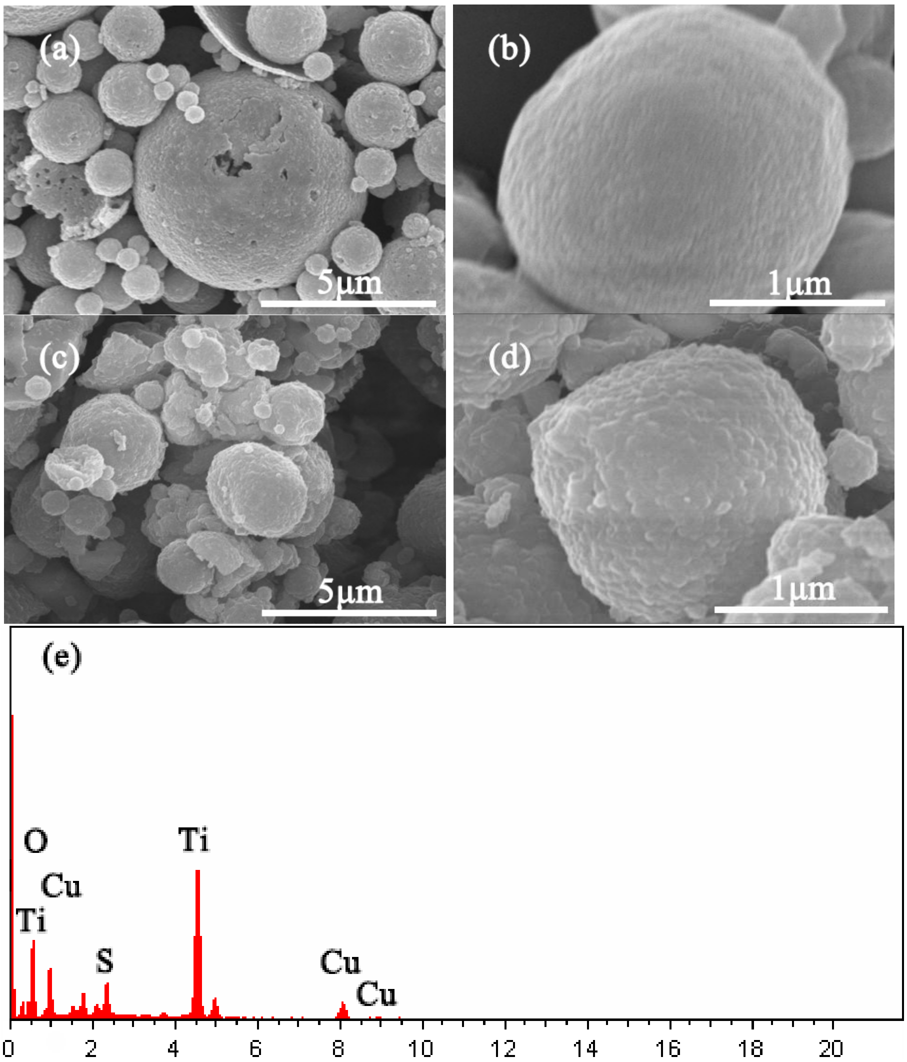

Figure 2. SEM images of LTO (a, b) and Cu_2S@LTO (c, d), and EDS spectrum of Cu_2S@LTO (e)

Figure 3 (a) is the charge and discharge curves of the first and eleventh cycles of the Cu_2S@LTO material in the ester electrolyte (LB301 electrolyte). Figure 3 (b) shows the cycle performance of the Cu_2S@LTO material during the first 30 cycles in the ester electrolyte (LB301 electrolyte). It can be seen from the figure that the specific capacity for the first discharge cycle is 206 mA hg^{-1}, the specific capacity for the first charge cycle is 188 mA hg^{-1}, the specific discharge capacity for the eleventh cycle is 88 mA h/g, and the specific charge capacity is 90 mA h/g. The first cycle coulomb efficiency is 91.26%. There are three potential platforms of 2.05 V, 1.65 V and 1.5 V in the discharge curve of the first cycle, and three potential platforms of 1.61 V, 1.91 V and 2.3 V are observed in the charging curve of the first cycle

[19]. During the eleventh cycle, there is one charging and discharging platform. These potential platforms correspond to the redox peaks in Figure 6 (d). The capacity of the Cu_2S@LTO material in the LB301 electrolyte rapidly decays during the first 10 cycles but is stable in the later period, and the cycle retention rate is 40%. This phenomenon is consistent with the properties of Cu_2S in ester electrolytes [18]. During the first 10 cycles of the Cu_2S@LTO material, the capacity of Cu_2S decays to 0, and only the LTO material retains capacity in the ester electrolyte during the later period.

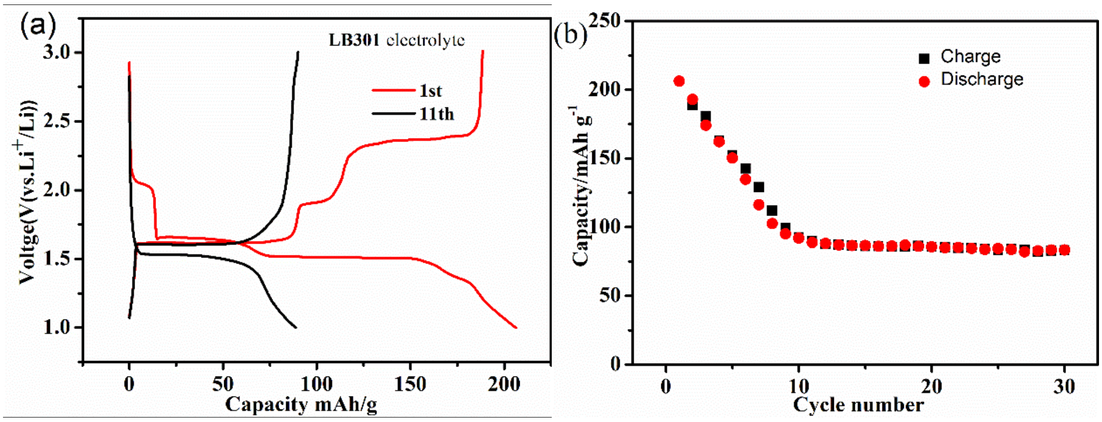

Figure 3. (a,b) Charge and discharge curves and cycle performance of Cu_2S@LTO in the LB301 electrolyte

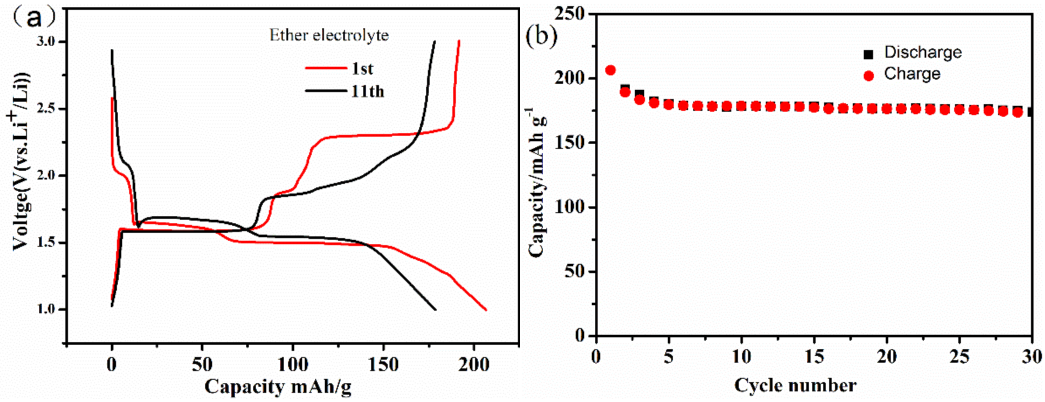

Figure 4. (a,b) Charge-discharge curves and cycle performance of Cu_2S@LTO in the ether electrolyte

Figure 4 (a) shows the charge and discharge curves of the first and eleventh cycles of the Cu_2S@LTO material in the ether electrolyte. Figure 4 (b) shows the cycle performance of the Cu_2S@LTO material during the first 30 cycles in the ether electrolyte. There are three potential platforms of 2.05 V, 1.65 V and 1.5 V in the first cycle of the discharge curve and three potential platforms of 1.6 V, 1.85 V and 2.3 V in the charging curve of the first cycle. During the eleventh cycle, the three potential platforms in the discharge curve do not change, and only two potential platforms of 1.6 V and 1.85 V remain in the charging curve. These potential platforms correspond to the redox peaks in Figure 6 (d).

As we can see from the diagram, the specific capacity for the first discharge cycle is 206.4 mA h/g, and the Coulomb efficiency is 92.88%. The discharge specific capacity of the eleventh cycle is 178.3 mA h/g, and the charge specific capacity is 178.6 mA h/g. The capacity retention rate for 30 cycles is 84%. It is proved that the Cu_2S@LTO material has a good cycle performance in ether electrolytes, because both Cu_2S and LTO materials have a good cycle performance in ether electrolytes.

Figure 5 (a) is the charge-discharge cycle diagram of Cu_2S@LTO in the ether electrolyte at a 10 C rate. The specific discharge capacity of Cu_2S@LTO during the first cycle is 131.5 mA h/g, the Coulomb efficiency during the first cycle is 106.1%, and the capacity retention rate after 100 cycles is 98.5%, proving that the Cu_2S@LTO material has a good cycle performance at 10 C. Figure 5 (b) is the rate performance graph of Cu_2S@LTO in the ether electrolyte. For 0.5 C, 1 C, 3 C, 5 C, and 10 C rate charges during the discharge cycles, the specific discharge capacities are 239, 200, 165, 155, and 135 mA h/g, respectively. In this process, the average Coulomb efficiency is above 98%. When the rate increased from 0.5 C to 10 C, the capacity retention rate is 56.5%. When the charge-discharge rate is restored to 0.5 C, the reversible capacity of the Cu_2S@LTO electrode material quickly recovers to 220 mA h/g. Thus, the Cu_2S@LTO electrode material exhibits a good cycle stability and rate performance in ether electrolytes.

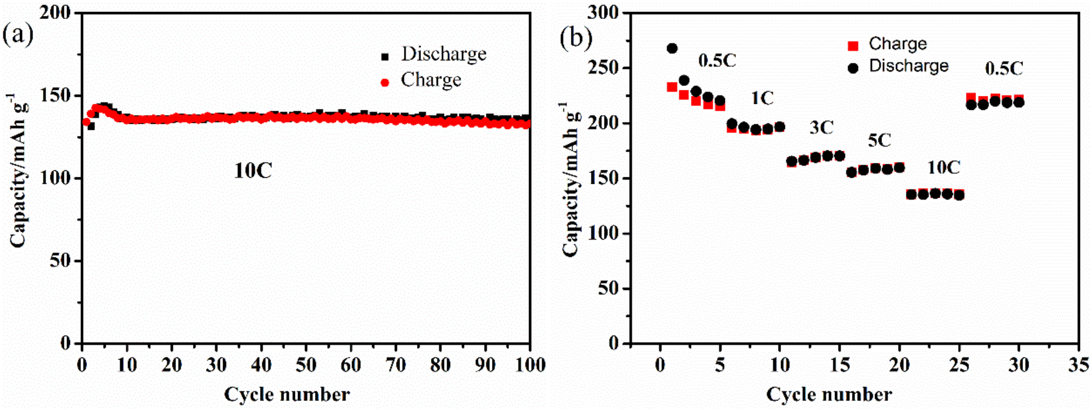

Figure 5. Cycle performance (a) and rate capabilities (b) of Cu_2S@LTO in the ether electrolyte

Figure 6 (a) and (b) are the CV curves of the commercial Cu_2S and LTO, respectively. Figure 6 (c) compares the first cycle CV curves of LTO and Cu_2S@LTO. Figure 6 (d) is the CV diagram of the first 5 cycles of Cu_2S@LTO. The comparison between the CV curve of the Cu_2S@LTO material in the ether electrolyte and the CV curve of the pure LTO material shows that there were many reduction peaks at 1.65 V and 2.1 V and many oxidation peaks at 1.85 V and 2.4 V. These many peaks all correspond to the lithium storage of Cu_2S. The Cu_2S@LTO material has three pairs of redox peaks in the first CV curve. The two reduction peaks at 1.65 V and 2.1 V correspond to the electrochemical reaction $Cu_2S + 2Li^+ + 2e \leftrightarrow Li_2S + 2Cu$. The two oxidation peaks at 1.85 V and 2.4 V belong to the corresponding electrochemical reaction $2CuS + 2Li^+ + +2e \leftrightarrow Li_2S + 2Cu_2S$.[20] The electrochemical properties of similar lithium ion anode materials are shown in Table 1. By comparing the data in the table, the lithium titanate prepared by this work has shown excellent electrochemical performance, especially the cycle stability.

The cycling stability characteristics of the LTO based electrodes are summarized in Table 1, which also compares them with the cycling stability characteristics previously reported for other LTO electrodes used as anodes in lithium-ion battery systems. At present, the modification of LTO is mainly carried out from two aspects. On the one hand, it is compounded with high-conductivity materials, such as copper, carbon and TiN [21, 22, 24, 25]. On the other hand, it is doped with transition metal ions to convert tetravalent titanium into trivalent titanium, thereby improving the conductivity [26, 27]. A very small part of the work uses metal oxides and titanium-based materials, such as tin oxide, but because these metal oxides have poor electrical conductivity and easily cause large volume expansion during energy storage, the improvement of electrochemical performance is not ideal [23]. Because copper-sulfur compound is a highly conductive semiconductor and has a small volume expansion during energy storage, it is an ideal energy storage material [16-18]. In this work, it is combined with cuprous sulfide to improve conductivity while increasing the specific capacity. In comparation, the as prepared Cu_2S@LTO in this work has a higher first specific capacity and better cycle stability. After 100 cycles, the specific discharge capacity is above 130 mAh/g with a high capacity retention rate of 98.5%.

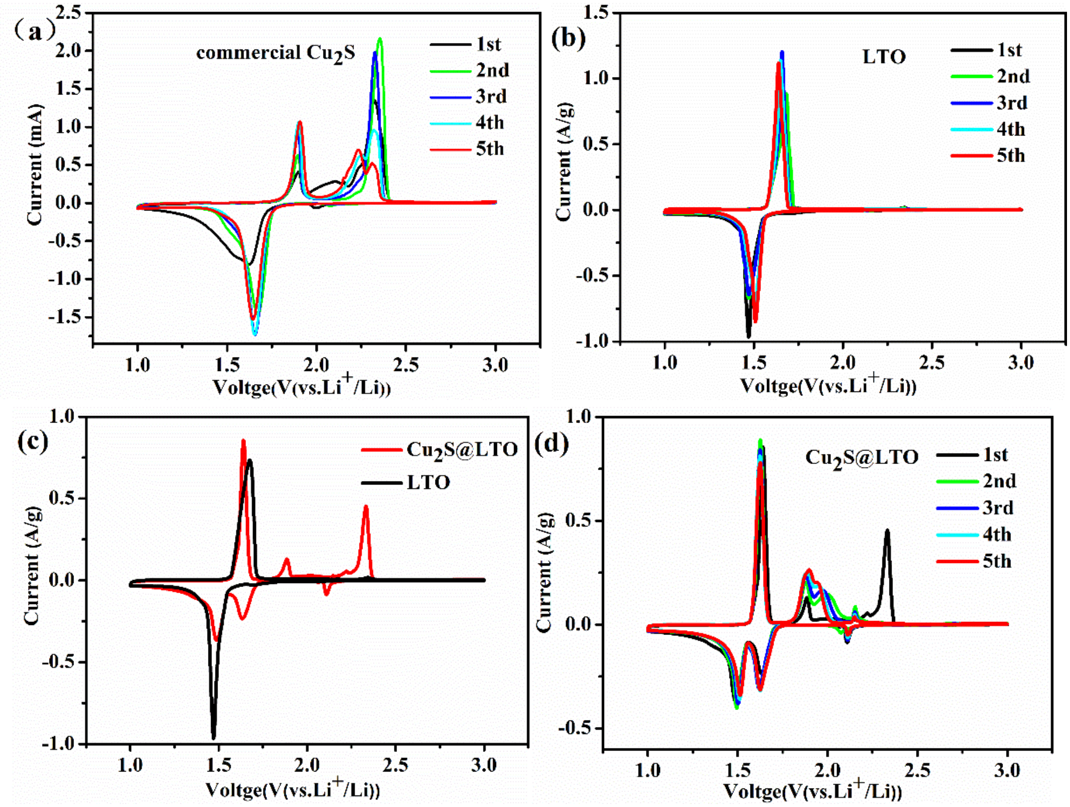

Figure 6. The CV curves of commercial Cu_2S (a) and LTO (b). The CV curves of LTO and Cu_2S@LTO (c). The CV curves of Cu_2S@LTO (d).

Table 1. This material has been compared with other materials

Electrode materials	First specific capacity/mAh/g	Cycle performance	Ref.
$Li_4Ti_5O_{12}/Cu_2S$	206	After 100 cycles, the specific discharge capacity is above 130 mAh/g with high capacity retention rate of 98.5%	This work
$Li_4Ti_5O_{12}/TiN$	173	After 100 cycles, the specific discharge capacity is 160.0 mAh/g	[21]
$Li_4Ti_5O_{12}/C$	172.2	After 20 cycles, the specific discharge capacity is 167.0 mAh/g	[22]
$Li_4Ti_5O_{12}/SnO_2$	476	After 16 cycles, he specific discharge capacity is 236 mAh/g	[23]
$Li_4Ti_5O_{12}/C$	168.8	After 100 cycles, the specific discharge capacity is 136.4 mAh/g	[24]
$Li_4Ti_5O_{12}/Cu$	209	After 60 cycles, the specific discharge capacity is 163.4 mAh/g	[25]
Sn-doped $Li_4Ti_5O_{12}$	135	After 100 cycles, the specific discharge capacity is above130 mAh/g	[26]
Ni-doped $Li_4Ti_5O_{12}$	162	After 50 cycles, the specific discharge capacity is above132 mAh/g	[27]

5. CONCLUSIONS

Aiming to solve the two major problems of lithium titanate, namely, poor conductivity and low capacity, this work comprehensively improves the specific capacity and conductivity of lithium titanate by coating with Cu_2S, a semiconductor material with a good conductivity. The spherical lithium titanate was synthesized by spray drying, Cu particles were then deposited on the LTO by the copper mirror reaction, and finally, sulfur powder was used for sulfidation. The obtained Cu_2S@LTO material maintains the spherical shape of the lithium nanotitanate micro-nano structure. The XRD and EDS results show that the prepared Cu_2S@LTO material has a high purity and high degree of crystallinity. By comparing the different electrochemical performances of the Cu_2S@LTO anode material in an ether electrolyte and ester electrolyte (LB301), it was found that the Cu_2S@LTO anode material had a better electrochemical performance in the ether electrolyte than in the ester electrolyte. In the ether electrolyte, the specific capacity for the first discharge cycle is 206.4 mA h/g, and the first cycle Coulomb efficiency is 92.88%. After 30 cycles, the capacity retention rate is 91%. Even at a high rate, the capacity retention rate after 100 cycles can still be maintained at 98.5%. The excellent electrochemical energy is due to the synergistic effect of Cu_2S and lithium titanate, which not only improves the specific capacity of the material but also effectively improves the electrical conductivity, thereby comprehensively improving the electrochemical storage performance of the battery.

ACKNOWLEDGMENTS

We gratefully acknowledge the National Natural Science Foundation of China (No. 21965017 and 51764029) and the Provincial Natural Science Foundation of Yunnan (No. 2017FB085 and 2018FB087).

References

1. Y. J. Zhang, H. C. Yan, J. M. Liu, X. Li, Y. Y. Zhang, *Int. J. Electrochem. Sci,* 15(2020)2894.
2. J. M. Liu, Y. H. Lu, R. X. Wang, Z. F. Xu, X. Li, *Int. J. Electrochem. Sci,* 15(2020)1571.
3. H. C. Yan, Y.Y. Zhang, Y. X. Wang, J.M. Liu, X. Li, Y.J. *Zhang, Ceram. Int.*, 45(2019)20796.
4. X. Li, X. Y. Zeng, T. Ren, J. B. Zhao, Z. Y. Zhu, S. G. Sun, Y. J. Zhang, *J. Alloys Compd.,* 787(2019)229.
5. Q. Wang, S. Yang, J. Miao, M. Lu, T. Wen, J. Sun, *Appl. Surf. Sci.*, 403(2017)635.
6. D. H. Long, M. G. Jeong, Y. S. Lee, *ACS Appl. Mater. Interfaces*, 7(2015)10250.
7. Y. Yang, B. Qiao, X. Yang, *Adv. Funct. Mater.*, 24(2014)4349.
8. B. Zhao, R. Ran, M. Liu, *Mater. Sci. Eng., R*, 2015, 98(2015)1.
9. C. P. Sandhya, B. John, C. Gouri, *Solid State Ionics.*, 20(2014)601.
10. Z. Yu, H. Xu, G. Zhu, D. Yan, A. Yu, *Appl. Surf. Sci.*, 368(2016)173.
11. J. Kim, J. Y. Kim, D. Pham-Cong, S. Y. Jeong, J. Chang, J. H, Choi, *Electrochim. Acta*, 199(2016)35.
12. Y. Zhang, Y. Meng, K. Zhu, H. Qiu, Y. Ju, Y. Gao, F. Du, B. Zhou, G. Chen, Y. Wei, *ACS Appl. Mater. Interfaces*, 8 (2016) 7957.
13. C. A. Triana1, C. G. Granqvist1 and G. A. Niklasson, *J. Appl. Phys.*, 119(2016)111.
14. L. J. Fu, K. Endo, K. Sekine, T. Takamura, Y. P. Wu, H. Q. Wu, *J. Power Sources*, 162(2006)663.
15. R. Dominko, M. Gaberscek, J. Drofenik, M. Bele, S. Pejovnik, J. Jamnik, *J. Power Sources*, 119(2003)770.
16. J. M. Liu, Y. H. Liu, R. X. Wang, Z. F. Xu, X. Li, *Int. J. Electrochem. Sci,* 15(2020)1509.
17. Y. J. Zhang, Y. T. Li, Q. Zhang, X. Li, Y.Y. Zhang. *Int. J. Electrochem. Sci,* 15(2020)2903.
18. Y. T. Li, Y. Y. Zhang, Y. X. Wang, X. Li, Q. Zhang, H.C. Y, X. S. Huang, H. K. Liu, Y. J. Zhang, *Electrochim. Acta*, 335(2020)135662.
19. C. H. Lai, K. W. Huang, J. H. Cheng, C. Y. Lee, B. J. Hwang and L. J. Chen, *J. Mater. Chem.*, 2020(10)6638.
20. F. Han, W. C. Li, D. Li and A. H. Lu, *Chemelectrochem*, 1(2014)733.
21. X. L. Zhou, R. A. Huang, Z. C. Wu, *Acta Phys. Chim. Sin.*, 26(2010) 3187.
22. J. Gao, X. Mu, J. J. Li, X. M. He, *Int. J. Inorg. Mater. International*, 27(2012) 253.
23. Y. Y. Wang, Y. J. Hao, Q. Y. Lai, J. Z. Lu, Y. D. Chen, X. Y. Ji, *Appl. Surf. Sci.*, 14 (2008) 85.
24. Z. Lin, W. Zhu, Z. Yang, Y. Yang, Y. Lin, Z. Huang, *J. Alloys Compd.*, 16(2016)232.
25. S. H. Huang, Z. Y. Wen, B. Lin, J. D. Han, X. G. Xu, *J. Alloys Compd.*, 457 (2008) 400.
26. B. Zhang, Z. D. Huang, S. W. Oh, J. K. Kim, *J. Power Sources*, 96 (2011) 10692.
27. J. Kim, S. W. Kim, H. Gwon, W. S. Yoon, Kisuk Kang, *Electrochim. Acta*, 54 (2009) 5914.